Biomass and Bioenergy 204 (2026) 108406

Contents lists available at ScienceDirect

Biomass and Bioenergy

journal homepage: www.elsevier.com/locate/biombioe

Catalytic pyrolysis of non-textile button components as a co-feedstock for bioenergy production

Samy Yousef [a,*], Justas Eimontas [b], Nerijus Striūgas [b], Mohammed Ali Abdelnaby [c]

[a] Department of Production Engineering, Faculty of Mechanical Engineering and Design, Kaunas University of Technology, LT-51424, Kaunas, Lithuania
[b] Lithuanian Energy Institute, Laboratory of Combustion Processes, Breslaujos 3, LT-44403, Kaunas, Lithuania
[c] Mechatronics Systems Engineering Department, October University for Modern Sciences and Arts-MSA, Giza, Egypt

ARTICLE INFO

Keywords:
Textile waste
Plastic buttons
Catalytic pyrolysis characteristics
Benzoic acid
Machine learning
Catalytic kinetic modelling

ABSTRACT

Recently, the co-pyrolysis of biomass and various types of plastic waste (PW) has shown great potential in improving H/Ceff ratio of biomass, making it a sustainable and competitive source of bioenergy, especially in the presence of catalysts. However, this strategy is limited by high contamination and the difficulty of sorting PW, requiring the development of another clean and uniform source of PW. In this context, this research presents polyester and nylon buttons (major part of non-textile components) as a new type of clean and sortable PW for this purpose. The experiments at this stage was focused on studying the catalytic pyrolysis of plastic buttons only by thermogravimetric analysis (TGA) coupled with Fourier transform infrared (TG-FTIR) and gas chromatography-mass spectrometry (GC/MS) to provide the basic data needed for future co-pyrolysis with biomass. The energy consumed during the reaction (Ea) and other catalytic pyrolysis characteristics over ZSM-5 zeolite catalyst were evaluated using kinetic models along with determination of their thermodynamic parameters. Also, an artificial neural network (ANN) algorithm was proposed to expect TGA properties of buttons at ambiguous heating parameters. The TGA results revealed that polyester sample can be decomposed in two stages up to 360 °C and 460 °C, while nylon sample decomposed in a single stage up to 490 °C. The TGA-FTIR analysis highlighted that carbonyl groups (polyester) and aliphatic hydrocarbons (nylon) are the main functional groups of polyester and nylon vapors. Meanwhile, benzoic acid (72.94 % at 20 min/°C) the main compound of nylon sample and 1,2-Benzenedicarboxylic acid (plasticizers) the main compound of polyester and its toxic styrene compound was completely removed. Finally, the Ea used in decomposition of buttons was estimated at 241.6–262.7 kJ/mol (polyester) and 165.6–173.4 kJ/mol (nylon). The suggested ANN model showed high potential in predicting the catalytic pyrolysis characteristics with $R > 0.98$. Based on these findings, plastic buttons can be used as a co-feeding hydrogen-rich source to biomass to enhance its H/Ceff ratio and aromatic compounds.

1. Introduction

Textile waste management (TW) is a major global concern facing the world in general and the European Union (EU) in particular, as the EU produces 12.7 million tons annually [1], which exceeds 7 million tons of 7 Mt CO_2 eq [2]. TW has also been recognized as a contributor to the generation of microplastics that threaten oceans and living organisms [3,4]. However, TW has a unique composition consisting of textile components (Ts: 95 wt%) and non-textile components (NTs: 5 wt%) [5]. Ts refers to fabrics, which are usually made of synthetic fibers (polyester, nylon), natural fibers (cotton, silk, rayon, viscose, etc.) or mixed fibers [6,7]. While NTs refer to trims that are used to decorate fabrics and add a touch of beauty [8]. This unique composition of textiles rich in many natural and petrochemical components has encouraged manufacturers to recover their components in the form of fibers or energy products and reuse in the production process, contributing to a more sustainable textile industry and the transition towards a circular, waste-free economy [9,10]. However, this vision faced some challenges related to collecting, sorting and dismantling TW before starting recycling them [11]. Therefore, the EU recently adopted new rules that require its members to address all these barriers, by developing TW collection, sorting, and disintegrate trims systems [1,12,13], thus

* Corresponding author.
E-mail address: ahmed.saed@ktu.lt (S. Yousef).

https://doi.org/10.1016/j.biombioe.2025.108406
Received 26 March 2025; Received in revised form 17 June 2025; Accepted 16 September 2025
Available online 25 September 2025

obtaining fabrics and NTs components ready for recycling.

Regarding to fabrics recycling, incineration is the traditional practice used to for energy recovery from Ts [14]. However, TW incineration suffers from several disadvantages relevant to emissions, excessive expenditure of energy, and resource depletion [15]. To avoid these disadvantages, some effective thermochemical methods using pyrolysis and gasification have been developed to transfer fabrics into energy resources (petroleum, coal, hydrogen-rich syngas, fuels, etc.) or fiber recovery [16–19]. Also, the chemical treatment using leaching, dissolution, and bleaching have been developed to extracted and purified fiber from fabrics [5,20]. In fact, all these processes showed high potential in Ts recycling with promising environmental and a socio-economic performance [21], and the remarkable thing is that all the treatments were performed on fabrics free of any NTs. This due to fact that the presence of NTs with fabrics complicates its recycling process and produces secondary materials with lower quality, competitiveness and compatibility. This complexity comes from the fact that NTs have different composition, shape and geometry which makes it difficult for them to mix uniformly with fabrics and decompose together [6,8]. Consequently, NTs and fabrics should be recycled separately. Buttons represents the major fraction of NTs, and are usually made of plastic or metal components [8]. Based on the current situation, the aged buttons are categorized into plastics and metallic components, and then acceptable standard are selected for reuse. The poor quality metal buttons are melted and repurposed in mining processed [22], whereas poor quality plastic buttons are discarded as part of municipal solid waste and typically incinerated, which suffers from many shortcomings as mentioned before [15]. Therefore, NTs including buttons are the missing link in TW recycling, which requires effective solutions. In this regard, two approaches have been recently developed. The first approach proposed the use of biodegradable buttons instead of undegradable materials to mitigate environmental burdens and reduce its waste accumulation [8,23], but its performance is still not satisfactory and needs further development.

While the second approach focused on recycling NTs using pyrolysis as an eco-friendly technology and converting it into original chemical compounds [24]. The research began by identifying the material composition of many commercial plastic buttons using Fourier transform infrared (FTIR) and the examination showed that polyester resin and nylon were the main materials of buttons. While the pyrolysis experiments were conducted on nylon and polyester resin buttons using thermogravimetric analyser (TGA) connected with FTIR and gas chromatography-mass spectrometry (GC/MS) to determine pyrolysis properties of buttons, their kinetics and decomposition pathway, and to investigate the composition of vapors. The results showed that pyrolysis successfully decomposed them into nylon and polyester buttons into caprolactam (40 %) and styrene (84 %) compounds, respectively. However, the production of caprolactam is still low, and increasing its production will inevitably bring high economic benefits [25]. On the contrary, despite pyrolysis showed high potential in styrene recovery, styrene is a toxic carcinogenic compound that must be cracked [26]. Therefore, both chemical compounds need future processing for upgrading them and achieve this goal. Although the catalytic pyrolysis of plastic buttons has not been addressed before, but this process is very common in this regard and the research in literary works have demonstrated that thermochemical (THC: catalytic pyrolysis) can help enhance the recovery of caprolactam (69 %) from nylon [27,28], and degrade styrene of organic part of wind turbine blade waste (polyester resin) turning into enriched aromatic chemicals (benzene, toluene, and ethylbenzene) over ZSM-5 zeolite catalyst [29]. Accordingly, this research aims to study the THC performance of polyester and nylon buttons over zeolite catalyst (ZSM-5 grade) using TGA, TG-FTIR, GC/MS systems for enhancing recovery of caprolactam compound and thermal cracking of styrene compound. The THC kinetic and thermodynamic parameters of buttons were also studied, and then an algorithm for predicting the thermal degradation was developed using artificial neural network (ANN).

2. Experimental and methodology

2.1. Feedstocks preparation

Polyester and nylon buttons were used in the current research as our previous research showed that both plastics are classified as commonly materials used in production of buttons after examining 14 commercial buttons [24]. The plastic buttons with the specific composition were bought from a local shop in Lithuania specializing in old fashions. Nylon and polyester batches were milled separately and subsequently sieved to produce fine powder with uniform distribution less than 500 μm. The elemental and proximate properties of buttons have been previously measured by our group and all parameters are summarized in Table (1) [24]. While zeolite catalyst (ZSM-5 grade) utilized in the present work as it showed a high performance in enhance the recovery of caprolactam from nylon material and eliminate on styrene of polyester resin [27–29]. The catalyst was provided by Sigma-12 Aldrich Corp, with all relevant specifications outlined here [30]. Each button sample was mixed with 20 wt% of ZSM-5 catalyst as this ratio has been reported as the optimum value in the literature which provides more caprolactam compound and breakdown styrene in the pyrolysis vapor [28,29], thus preparing the ZSM-5/nylon and ZSM-5/polyester feedstocks. The ZSM-5 zeolite catalyst used in the experiments has the following properties: SiO_2/Al_2O_3 molar ratio = 38, pore volume ≥0.25 mL/g, bulk density = 0.72 kg/l, specific surface area ≥250 m^2/g, crushing strength ≥98 N/cm^2, attrition <1 wt%, and pore size = ~5 Å [31]. In order to prepare batches of catalyst/button with a uniform mixture, the ZSM-5 granules were ground into fine particles using an electric mixer for 10 min, and then the catalyst particles were mixed with the button powder for an additional 10 min. Finally, a flowchart of the catalytic pyrolysis experiments of plastic buttons and its kinetic analysis is shown in Figure (1).

2.2. Thermogravimetric analysis

The thermal degradation profiles of polyester and nylon buttons over ZSM-5 catalyst were observed using a TGA instrument (NETZSCH model). TGA testing was conducted on 8–10 mg of each button batch in an oxygen-free, nitrogen-filled atmosphere with 60 ml min^{-1} (flow rate). The degradation values were recorded from ambient temperature to 900 °C under varying heating conditions, in particular 10, 20 and 30 °C/min, allowing modelling of catalytic pyrolysis kinetics of each button batch [32]. This variety of heating conditions can also help to observe its effect on the abundance and composition of the released catalytic pyrolysis vapors. The mass loss of button samples was captured with rising the catalytic pyrolysis temperature followed by plotting TGA profiles for each samples at the specified heating conditions. After that, TGA data for each sample were derived using Proteus software, thus generate the necessary data required to plot the derivative thermogravimetric (DTG) patterns of buttons samples. Finally, the catalytic pyrolysis efficiency of plastic buttons was estimated based on the thermal decomposition index (CPI) formula which was described using **Eq.** [1, 33].

$$CPI = \frac{(-R_{max}) \times (-R_{avg}) \times M_f}{T_{int} \times T_{peak} \times \Delta T_{1/2}} \quad (1)$$

2.3. Catalytic pyrolysis vapors analysis

The catalytic pyrolysis vapors emitted from the decomposition of nylon and polyester buttons in the main decomposition region (based on TGA-DTG analysis) were monitored using TG-FTIR, GC/MS. The TG-FTIR device (Bruker Tensor 27, Germany) was adapted to examine the chemical groups of the emitted vapors through sent it directly to the FTIR unit using an infrared gas cell. While GC/MS device (Agilent 7890A

Table (1)
Elemental and proximate analysis of nylon and polyester buttons [24].

	Elemental analysis (wt%)					Proximate analysis (wt%)			
Parameter	Carbon	Hydrogen	Nitrogen	Sulfur	Oxygen	Moisture	Volatile matter	Fixed carbon	Ash
Nylon	90.45	7.70	0.00	0.00	1.85	0.33	99.67	0.00	0.00
Polyester	68.27	6.05	0.00	0.00	25.68	1.15	93.18	5.34	0.33

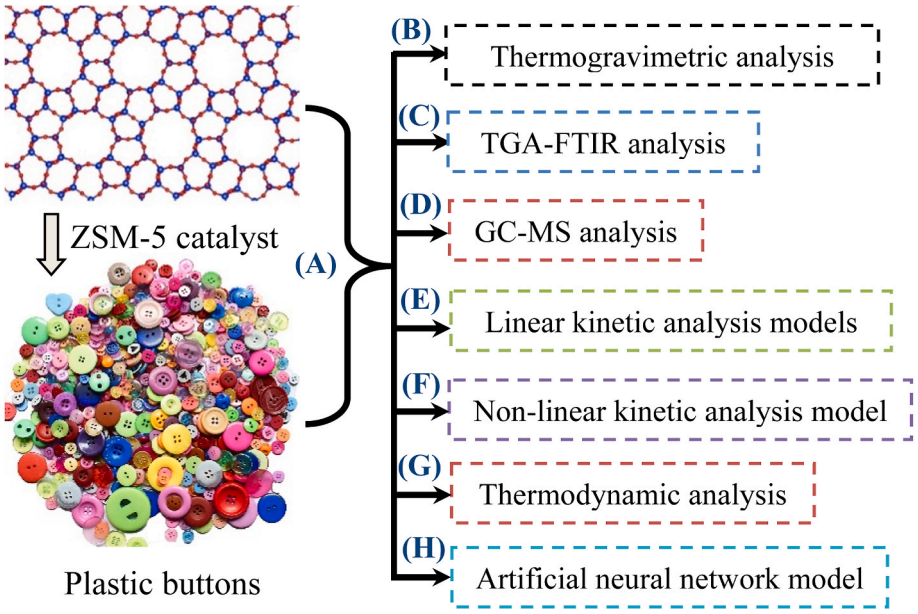

Figure (1). Flowchart of catalytic thermochemical experiments and analysis of plastic buttons.

GC coupled with a 5975 MSD) was applied to assess the chemical structure of the catalytic pyrolysis vapors and their abundance at 20 psi in helium ambient has purity >99.999 % [34].

2.4. Catalytic pyrolysis kinetic and thermodynamic analysis

The kinetics of catalytic thermal decomposition of nylon and polyester buttons were computed using model-free methods and nonlinear models under the known heating conditions mentioned above. These traditional modelling methods can provide more data related to the energy consumed during the reaction (Ea: activation energy) that can be used to describe degradation mechanism of nylon and polyester buttons over ZSM-5 catalyst [35]. Since there are many traditional modelling methods in the literature, choosing the appropriate approach is a matter of debate, thus kinetic was studied in the current research using Kissinger Akahira Sunose (KAS), Flynn Wall Ozawa (FWO), Friedman, and Vyazovkin methods, which are among the most commonly used linear and advanced nonlinear kinetic techniques, then select the best models that reach the maximum value of coefficient of determination parameter (R^2) [36,37]. The KAS, FWO, and Friedmann models are marked by its minimalism as they do not rely on any presumptions and consider decomposition to take place in a single-step reaction [38]. While, Vyazovkin model (as a nonlinear approach) assumes that the feedstocks composed of several of elements decompose in parallel reactions [39]. Descriptions of the formulas of these models and R^2 parameter are enumerated in Table (2) [40,41].

Finally, the thermodynamic parameters of the catalytic pyrolysis of nylon and polyester buttons, including enthalpy (ΔH), Gibbs free energy (ΔG), and entropy (ΔS) factors, were calculated based on equations [7–9]. Where $K_B = 1.3819 \times 10^{-23}$ J/K, R = 8.314 J/mol K, A (s^{-1}) is the pre-exponential item, Tm is the maximum degradation temperature (DTG curves), and h = 6.6269×10^{34} Js [33].

Table (2)
Kinetic expressions used in the study of catalytic thermochemical of buttons.

Eq. No.	Model	Expression	Slop formula
2	KAS	$\ln\left(\frac{\beta}{T^2}\right) = \ln\left(\frac{AR}{Eag(y)}\right) - \frac{-Ea}{RT}$	-Ea/R
3	FWO	$\ln\beta = \left(\frac{\ln AEa}{Rgy}\right) - 5.335 - \frac{1.0516Ea}{RT}$	−1.0516Ea/R
4	Friedman	$\ln\left(\frac{\beta dy}{dT}\right) = \ln(Af(y))\left(\frac{-Ea}{RT}\right)$	-Ea/R
5	Vyazovkin	$(y) = \int_0^{\alpha}\frac{dy}{f(y)} = A\int_0^{t}\exp(-E/RT)dt$	
6	Definition of Y-axis of nonlinear plot	$\ln\left\{\frac{\beta_i}{T_{y,i}^2\left[h(x_{y,i}) - \frac{x_{y,i}^2 e^{x_{\alpha,i}}}{x_{y,i-0.1}^2 e^{x_{y,i-0.1}}}h(x_{y,i-0.1})\right]}\right\}$	

$$\Delta H = Ea - RT_m \quad [7]$$

$$\Delta G = Ea - RT_m \ln\left(\frac{K_B T_m}{hA}\right) \quad [8]$$

$$\Delta S = \frac{\Delta H - \Delta G}{T_m} \quad [9]$$

2.5. Artificial neural network modelling

Thermal prediction process of nylon and polyester buttons was designed using artificial neural network algorithm and developed using MATLAB® software. The neural network architecture (neural cell) of the algorithm was built using three layers (input, hidden, and output) and

Levenberg-Marquardt (LM) for neural network optimization. In order to accurately simulate the catalytic pyrolysis of plastic buttons, a feed-forward neural network was trained via the LM algorithm, which is highly efficient in handling nonlinear regression relationships such as those found in TGA data [42]. The thermal decomposition of the buttons was controlled by multiple overlapping interactions resulting in nonlinear and multivariate dependencies during the conversion process and its activation energy. The LM algorithm can be used as a second-order optimization model to capture the variation in activation energy and smooth its values. The model was trained on 190 experimental points based on random data division and structured into three stages: 70 % allocated for training, 15 % for testing, and another 15 % for validation [29]. Automatic early stopping was implemented through automatic checks, preventing overfitting. The catalytic pyrolysis temperature, heating condition, and conversion rate were adopted to defined the input layer, while, the weight loss was the main parameter used to defined the output layer. Whereas, the hidden layer was described as a non-linear transfer function formula estimated based on trial-and-error method. This layer was optimized to obtain the maximum R2 value [43]. To optimize the developed AN algorithm, several key training parts were evaluated, including mean square error (MSE), root mean square error (RMSE), mean absolute error (MAE), mean bias error (MBE), and R^2. The refined ANN model was applied to forecast the TGA degradation features of plastic buttons at unknown heating parameter (at 25 °C/min).

3. Results and discussion

3.1. TGA analysis of plastic buttons

Figure (2) displays TGA and DTG descriptions of polyester and nylon buttons over ZSM-5 catalyst and their disintegration traits. The TGA curve of polyester button batch has heat endurance up to 220 °C with very low weight loss (<2 wt%) due to moisture evaporation (Figure (2A)). Subsequently, significant decreases were observed up to 360 °C (19 wt%) and 460 °C (59 wt%). In case of nylon button (Figure (2B)), the sample showed resistance to thermal degradation up to 400 °C (3 wt%) due to the loss of its moisture content and evaporation of residual chemicals subsequent to sole decomposition region extending to 490 °C (81 wt%). Compared to the pyrolysis of buttons results, which produced almost no solid carbonaceous formation (solid residue) phase [24], the catalytic pyrolysis of buttons showed a significant presence of this fraction, reaching 20 wt%. This part refers to ZSM-5 catalyst used in catalytic conversion and due to its excellent thermal stability, it remains in the remaining solid part. On the other hand, the DTG curve of polyester button showed almost a single degradation region accompanied by a slight step as the TGA profiles showed two stages of degradation (Figure (2C)). While the DTG curve of nylon button showed a very sharp degradation peak which is consistent with its TGA results (Figure (2D)). It was evident from data that the intensity and sharpness of DTG peaks of polyester and nylon buttons gradually increased with increasing heating rate, which resulted in enhanced rate of heat transfer and it's the transfer of heat between buttons molecules, and then their complete decomposition [44,45]. Eventually, all the catalytic thermochemical characteristics of plastic buttons under specified heating rates were derived from the TGA and DTG diagrams, and then presented in Table (3).

3.2. TG-FTIR analysis

The emitted vapors from the catalytic thermochemical process of polyester and nylon button batches were analysed via 2D/FTIR and their

Table (3)
Catalytic thermochemical properties of polyester and nylon buttons.

Sample	Polyester button			Nylon button		
Heating rate (°C/min)	10	20	30	10	20	30
T_{int} (°C)	192	198	200	340	374	369
T_{peak} (°C)	367	380	397	419	435	436
R_{max} (%/min)	8.68	14.93	31.48	20.12	37.27	62.31
R_{avg} (%/min)	0.933	1.711	2.822	0.980	1.941	3.003
M_f (%)	19.82	26.61	19.20	15.82	16.71	13.94
ΔT1/2	67	72	68	36	37	36
CPI (%3 °C^{-3} min^{-2})	3.40E-05	1.25E-04	3.16E-04	6.08E-05	2.01E-04	4.50E-04

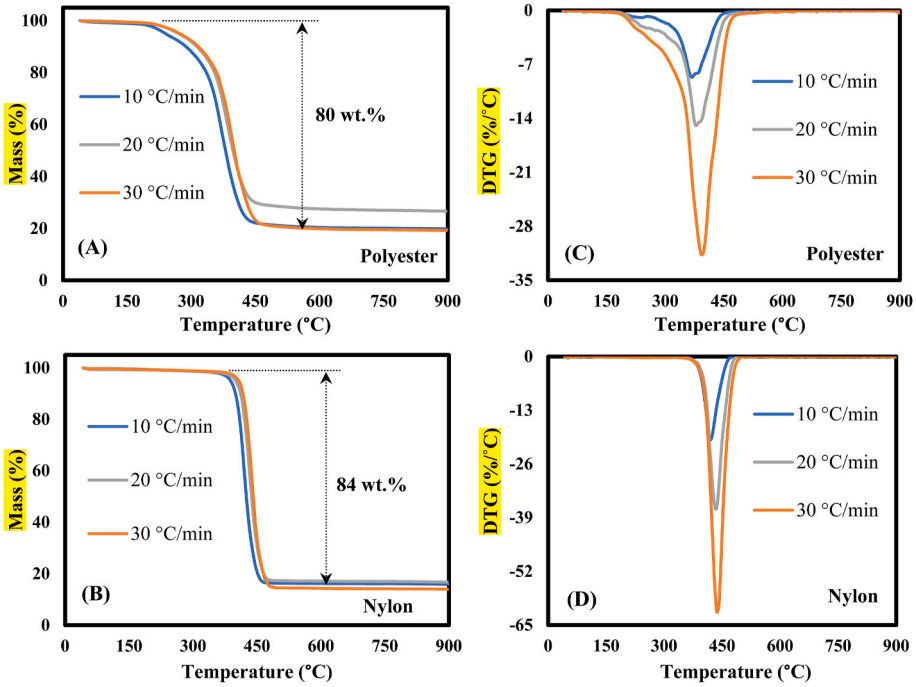

Figure (2). A,B) TGA profiles and C,D) DTG curves of polyester and nylon buttons.

patterns are displays in Figure (3). According to FTIR data, the vapors evolving from polyester sample consist of three main functional groups distributed in this way based on their intensity; carbonylic C=O groups at 1810 cm^{-1}, aromatic hydrocarbons at 906 cm^{-1}, C–O stretching vibrations at 1261 cm^{-1}, and C–H bond along with C=O stretching 2358 cm^{-1}. Also, some weak intensity groups at 3500 cm^{-1} (hydroxy (O–H)), 3000 cm^{-1} (aliphatic hydrocarbons), 1107 cm^{-1} (C–O–C stretching), and 700 cm^{-1} (aromatic hydrocarbons). In the case of nylon buttons, the emitted vapors were quite different compared to the polyester sample, where the high intensity groups were noticed that at 3085 cm^{-1} (aliphatic hydrocarbons), 650-900 cm^{-1} (aromatic hydrocarbons), and 1498 cm^{-1} (alkanes (-CH_3)) along with a minor CO_2 peak at 2337 cm^{-1} and carbonylic (C=O) functional group at 1620–1886 cm^{-1}. It was pointed out that the intensity of all FTIR bands increased as the heating rates were raised and the produced heating flux as a results of improve the heat transfer button the plastic molecules what enhances the degradation process into lighter hydrocarbons and peak absorbance [44,45]. Besides its contribution in eliminate the undesired reactions, which lead to developed smoother spectra as displayed in 3D/FTIR measurements. These FTIR patterns of the vapors obtained from both button samples in the present research are very similar to the vapors obtained from typical pyrolysis treatment [24]. However, the peak absorption of carbonyl groups at 1810 cm^{-1} (polyester) and aliphatic hydrocarbons at 3085 cm^{-1} (nylon) were significantly increased compared to those obtained from typical pyrolysis. Based on these results, the catalytic pyrolysis can promote aliphatic hydrocarbons and C=O carbonyl groups, which can be verified through GC/MS analysis, as outlined in the following section.

3.3. GC/MS analysis of the evolved catalytic pyrolysis products

Figures (4,5) exhibits the GC/MS spectra of the vapors rising from the catalytic thermochemical of polyester and nylon button batches, respectively. The identification of the synthesized compounds and their abundance at varying heating rates are presented in Tables (4,5). The GC/MS analysis (Figure (4)) showed that the catalytic pyrolysis could reduce the abundance of styrene by up to 14.16 % (at 20 min/°C) and 7.14 % (at 30 min/°C). At 20 min/°C, styrene decomposes into several compounds such as 1,2-hydrazine dicarboxamide (66.26 % at 20 min/°C), while at 30 min/°C it decomposes into 1,2-benzenedicarboxylic acid (38.97 %), benzoic acid (24.44 %), and benzene, 1,1'-(1,3-propanediyl) bis- (18.63 %). While the lowest heating rate succeeded in completely removing styrene compound which was strongly present in the pyrolysis vapor (84.54 %) [24]. Where styrene compound was decomposed into several compounds such as 1,2-benzenedicarboxylic acid (19.97 %), benzene, 1,1'-(1,3-propanediyl)bis- (13.63 %), 1,1':3′,1″-terphenyl, 5′-phenyl- (14.26 %), etc. The reason for this is that the low heating rate brings about increasing in the retention time of buttons inside the analytical reactor, which contributes to the decomposition of the entire styrene compound into other chemical compounds [29,46]. In the case of the nylon sample, its pyrolysis process showed that it could be decomposed into caprolactam (40.30 %) [24], while in the present case, catalytic pyrolysis significantly reduces its content in the range of 4.65–5.97 % and benzoic acid replaces it up to 72.94 % at 20 min/°C. In fact, there are several industrial methods for the production of caprolactam, one of which is a toluene-based process developed by Snia Viscosa in 1960 [47]. Caprolactam can be produced in this way using catalytic oxidation of toluene to produce a benzoic acid-rich liquid phase which then undergoes hydrogenation, nitrosodecarboxylation and rearrangement process and further purification to prepare the final product [47,48]. Based on that, the recovered benzoic acid was obtained from the original chemicals used in the production of caprolactam itself. In fact, these results are inconsistent with those in the literature which have shown that catalytic pyrolysis can help enhance the recovery of caprolactam (69 %) [27,28], due to the different composition and shape (fibres produced by spinning or extrusion) of the feedstocks used in the experiments, in particular textile waste and fishing nets. These results demonstrate that catalytic pyrolysis can be used to decompose styrene and caprolactam (main chemical compounds of polyester and nylon buttons) into their original chemical compounds or other value-added chemicals can be used as chemicals and plasticizers [49,50].

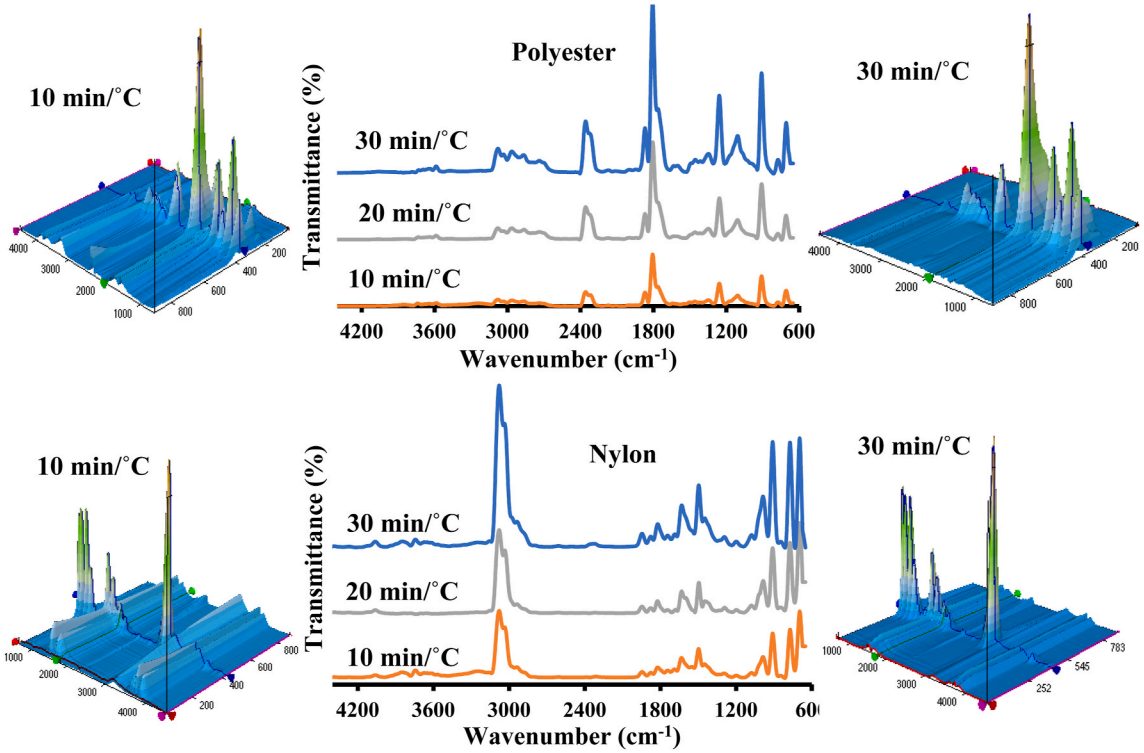

Figure (3). (2-3D)/FTIR bans of the emitted vapors from catalytic thermochemical treatment of plastic button samples.

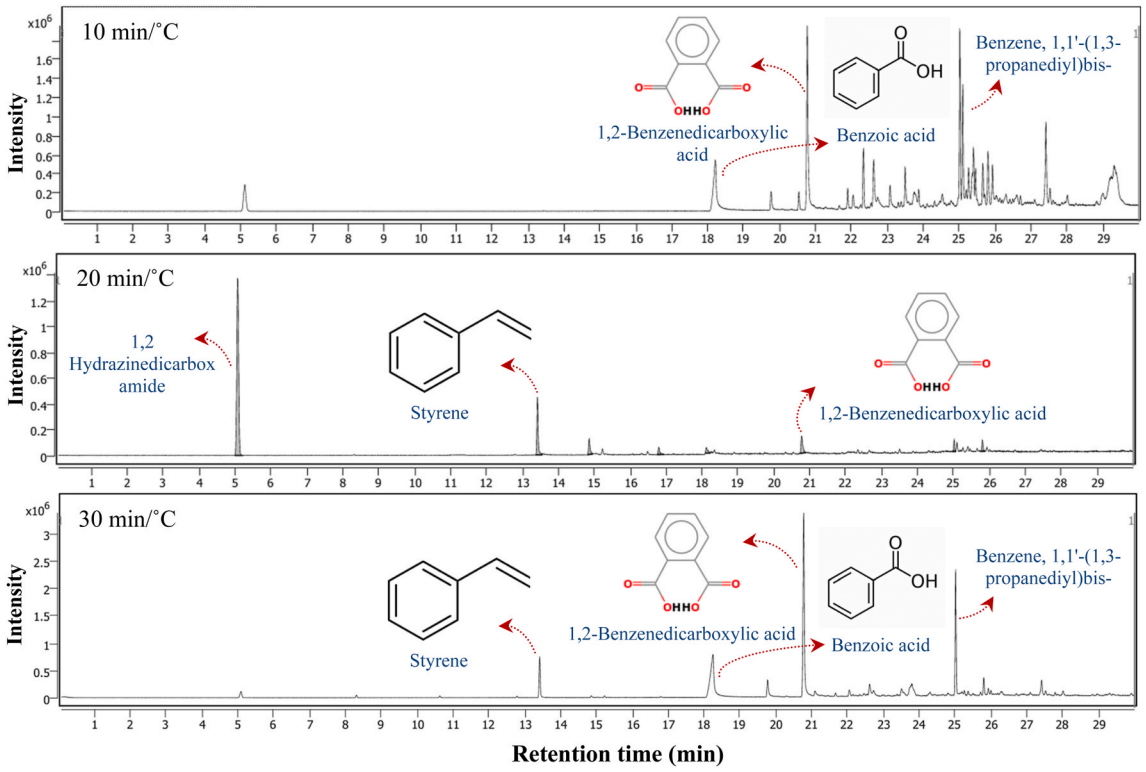

Figure (4). GC/MS spectra of the emitted vapors from pyrolyzed polyester button samples.

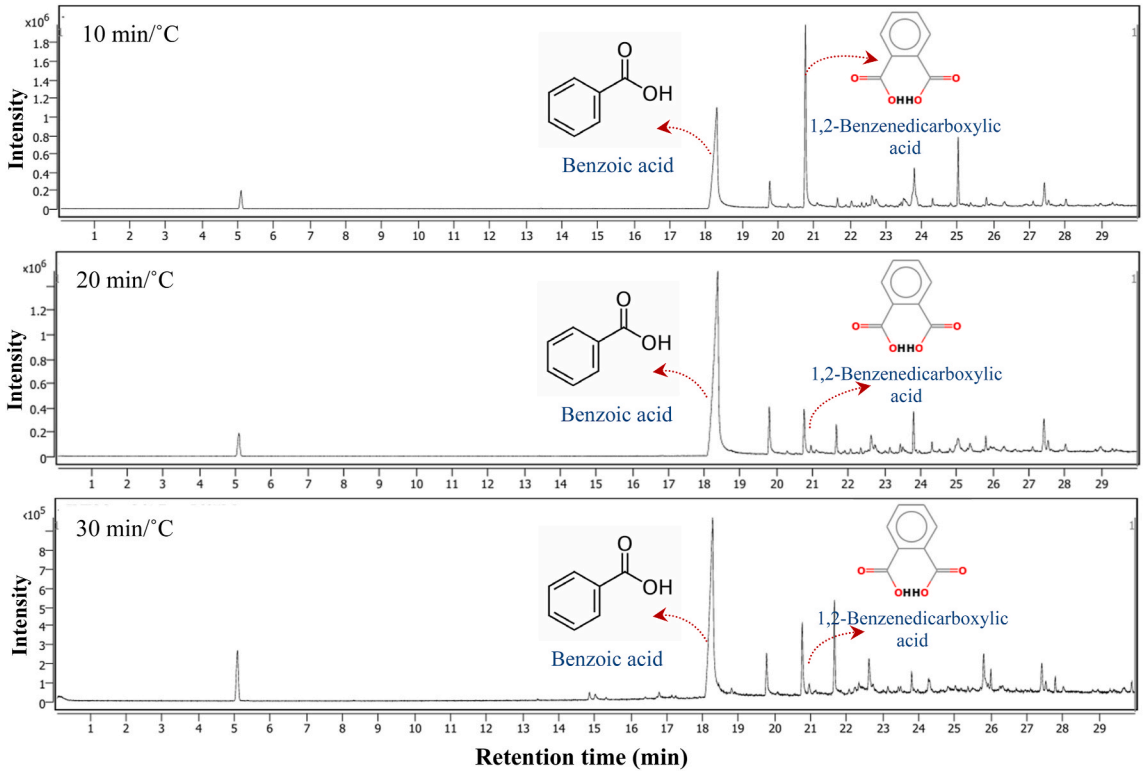

Figure (5). GC/MS spectra of the emitted vapors from pyrolyzed nylon button samples.

3.4. Catalytic pyrolysis mechanism of plastic button products

As shown above, each sample of plastic buttons contains many sub-components (resin, hardener, plasticizer) and many chemicals used during the different manufacturing process. All of these elements decompose simultaneously or sequentially during catalytic pyrolysis (including radicals reaction, cyclization, root rearrangement, and developing of aromatic compounds) [51], making its mechanism a

Table (4)
GC/MS characteristics of catalytic thermochemical vapors of polyester button samples.

10 min/°C			20 min/°C			30 min/°C		
Time (min)	GC Compounds	Area (%)	Time (min)	GC Compounds	Area (%)	Time (min)	GC Compounds	Area (%)
5.125	Alanine	5.03	5.078	1,2 Hydrazinedicarboxamide	66.26	13.418	Styrene	7.14
18.211	Benzoic acid	12.38	13.418	Styrene	14.16	18.248	Benzoic acid	24.44
20.768	1,2-Benzenedicarboxylic acid	19.97	14.860	Benzaldehyde	4.61	19.768	Caprolactam	4.18
25.013	Benzene, 1,1'-(1,3-propanediyl)bis-	13.63	16.796	Acetophenone	2.25	20.779	1,2-Benzenedicarboxylic acid	38.97
25.095	1,2-Diphenylcyclopropane	9.89	18.122	Benzoic acid	2.13	23.792	Cyclohexane, 1,3,5-triphenyl-	6.64
25.394	1H-Benzimidazole, 2 phenyl-, 3-oxide	7.45	20.768	1,2-Benzenedicarboxylic acid	5.88	25.013	Benzene, 1,1'-(1,3-propanediyl)bis-	18.63
27.408	.beta.Phenylpropiophenone	8.74	25.017	Benzene, 1,1'-(1,3-propanediyl)bis-	2.25			
29.221	1,1':3′,1″-Terphenyl, 5′-phenyl-	8.64	25.799	Naphthalene, 1,2,3,4-tetrahydro-2-phenyl-	2.46			
29.310	1,1':3′,1″-Terphenyl, 5′-phenyl-	14.26						

Table (5)
GC/MS characteristics of catalytic thermochemical vapor of nylon button samples.

10 min/°C			20 min/°C			30 min/°C		
Time (min)	GC Compounds	Area (%)	Time (min)	GC Compounds	Area (%)	Time (min)	GC Compounds	Area (%)
5.095	Alanine	3.59	5.098	Alanine	3.96	5.094	Acetic acid, 2-(N-methyl N phosphonatomethyl)ami no-	8.17
18.306	Benzoic acid	46.38	18.367	Benzoic acid	72.94	18.272	Benzoic acid	57.05
19.782	Caprolactam	4.65	19.796	Caprolactam	5.97	19.772	Caprolactam	5.42
20.768	1,2-Benzenedicarboxylic acid	27.23	20.762	1,2-Benzenedicarboxylic acid	5.39	20.761	1,2-Benzenedicarboxylic acid	8.46
23.496	Benzene, (2 chloropropyl)	2.45	23.796	Hydantoin, 5-ethyl-5- phenyl-, (.+/−.)-	3.63	21.656	Biphenyl	8.26
23.796	Benzene, (1- hexylheptyl)-	4.31	25.030	2,5 Dimethylbenzophenone	3.96	22.612	Phthalimide	4.04
25.013	Benzene, 1,1'-(1,3 propanediyl)bis-	7.63	27.411	.beta. Phenylpropiophenone	4.16	25.799	Benzonitrile, m- phenethyl-	5.46
27.408	.beta. Phenylpropiophenone	3.76				27.408	.beta.- Phenylpropiophenone	3.14

cumbersome and difficult to understand process. To address the complexity of this reaction and better understand the mechanism of the current research, the mechanism pathway characterized by TGA data and the identifications of key compounds through GC/MS measurements. The description focused on the TGA features of polyester button samples at 10 min/°C (which successfully removed all styrene) and the TGA features of nylon button samples at 20 min/°C which decomposed caprolactam to its original chemistry (benzoic acid) based on GC/MS measurements and the schematic of the mechanism is provided in Figure (6). As revealed in the scheme, nylon batch showed greater resistance to heat up to 400 °C, whereas polyester batch exhibited lower resistance up to 220 °C resulting from moisture and other residual chemicals (left during production) evaporation. Then, the complex molecules of the nylon (360 °C) and polyester (420 °C) buttons began to dismantle into smaller molecules with low crystally [52]. As the catalytic process progresses at the set temperature, the smaller molecules decompose back into their original chemical forms, in particular styrene (polyester) and caprolactam (nylon) [53–55]. The high acidity and large active sites of the ZSM-5 catalyst used help break down these compounds into the key chemicals used in their production, especially 1, 2-Benzenedicarboxylic acid (polyester) and benzoic acid (nylon) [47, 50]. The production of caprolactam and benzoic acid was enhanced through three steps. The first step is acid activity, where ZSM-5 has high Brønsted and Lewis acidic sites. Brønsted sites (OH groups) can help speed up the reaction of breaking down plastic buttons into smaller molecules, while Lewis sites resulting from extra-framework aluminium of the catalyst are key in dehydrogenation reactions and rearrangement of smaller molecules into parent compounds [56]. Second step is shape selectivity, ZSM-5 has a porous structure with straight and tortuous open channels that allow these small molecules to diffuse so that

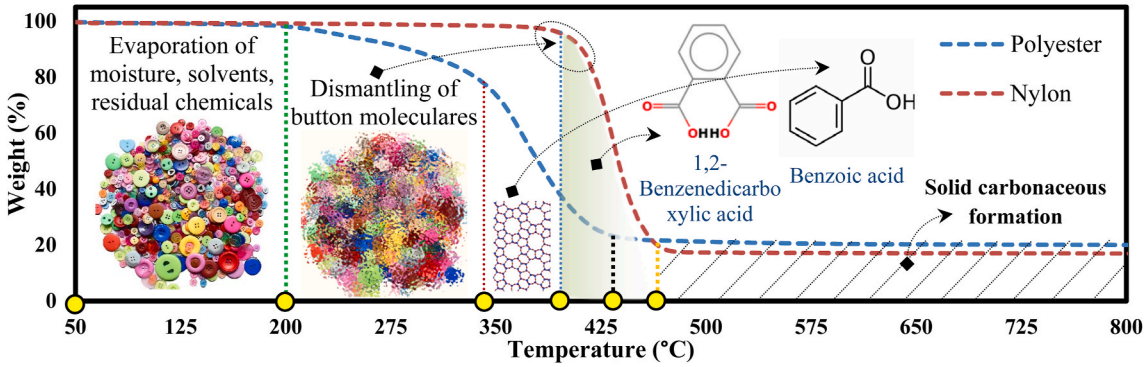

Figure (6). Mechanism of plastic buttons catalytic pyrolysis.

intermediates are trapped within its pores, favouring aromatization or ring closure, and then selecting the desired compounds [57]. Third step is the synergistic effects, where both acidity and selectivity of ZSM-5 has a synergistic action can be summarized as the acidic sites activate the reactants and catalyse them toward monocyclic aromatics over poly-aromatics through dehydrogenation and oligomerization reactions, while pore structure promote the selectivity of desired compounds and prevents excessive growth of aromatic substances, especially benzoic acid and 1,2-benzenedicarboxylic acid [58]. While the final stage of the reaction refer to solid residue (char mixed with catalyst that has high thermal resistance [29,59]) and this stage is called solid carbonaceous formation [60]. It was observed that the decomposition of styrene and caprolactam occurs at a low heating rate of less than 20 °C/min because the low heating rate results in increased retention time allowing the heat flux to diffuse and exchange between buttons molecules and achieve complete decomposition [61–63]. In addition, the long retention time increases the interaction with ZSM-5 catalyst, which helps it to complete dehydrogenation and oligomerization reactions and select the desired compounds as described above [27]. While the high heating rate helps in the formation of heavy hydrocarbons mostly resulting from incomplete decomposition along with the production of more residues [64].

3.5. Kinetic analysis

In order to compute the Ea of plastic button sample consumed during the catalytic pyrolysis for every rate of conversion (y) applying KAS, FWO, and Friedmann approaches, the fitting curves (Figure (7)) were drawn for each model based on the formulas given in Table (2) at each y in the ranges 0.1–0.9 through the following relations: ln (β/T^2) against 1/T (KAS model), ln(β) against 1/T (FWO), and ln (dy/dt) against 1/T (Friedmann) as plotting in Figure (7). This was followed by extracting the slope of each model based on the slope formulas listed in the same table (considering R = 8.31 JK^{-1} mol^{-1} [65]), thus estimating the Ea value at the reported conditions and the distribution of the calculated Ea and its values are presented in Figure (8) and Table (6). The fitted KAS and FWO curves show almost straight and parallel lines, especially after y = 0.2 until finishing the catalytic conversion process because at the beginning of the transformation it is usually accompanied by simultaneous and parallel interactions that are difficult to predict and fade away as the transformation progresses, then these reactions combine together, reducing the complexity of the reaction, and predicting a high R^2. While Friedmann curves are chaotic due to their high sensitivity to noisy data, resulting in random lines of fit [66,67]. Based on the fitted curves and their regressions, the average Ea of the polyester buttons were estimated to be 241.6 kJ/mol (KAS), 259.6 kJ/mol (FWO), 262.7 and KJ/mol (Friedman). On the other hand, the average Ea of nylon buttons were 165.6 kJ/mol (KAS), 172.8 kJ/mol (FWO), and 173.4 kJ/mol (Friedman) with high R^2 in the range of 0.98–0.99 (average value) for both button samples. This means that the catalytic pyrolysis of nylon buttons can reduce their degradation complexity as its typical pyrolysis was set to 156–201 kJ/mol. While the catalytic pyrolysis of polyester buttons has increased the complexity of the reaction because they contain many substances that require more Ea to decompose, as its pyrolysis Ea was set to be 152–202 kJ/mol [24]. Finally, the Ea of the plastic buttons was calculated again using Vyazovkin model built using MATLAB, followed by running it at 200 kJ/mol (as an starting point), then optimizing the algorithm until the Ea values became similar after several iterations. This goal was achieved after four iterations and their values are represented in Table (7). In this way, the average Ea was found to be 251 kJ/mol (polyester) and 165 kJ/mol (nylon) with R2 more than 0.98. Based on that Vyazovkin curves for both button samples were fitted (Figure (7)). It is apparent that, KAS and Vyazovkin models provide closely aligned Ea values with high R^2 making them suitable for simulating the catalytic pyrolysis of plastic buttons. Finally, the thermodynamic parameters of polyester button and nylon buttons were calculated at 10 min/°C and 20 min/°C, respectively, which successfully removed all styrene and decomposed caprolactam to benzoic acid as described above and all these parameters are shown in Table (8). The analysis showed that the ΔS and ΔH parameters had negative values, meaning that the reaction turned into an exothermic, more stable reaction, releasing heat to the surrounding environment with less randomness and organized small molecules combined with synthesized structured components [68].

3.6. Artificial neural network analysis

The TGA curves of polyester and nylon button samples were predicted using the built ANN algorithm at 25 °C/min as unknow parameter. The three hidden layers (3 × 5 × 1) are proven to be more reliable for the algorithm. These layers represent the structure of the feedforward artificial neural network model used to model the thermal degradation behavior of buttons, specifically the input layer containing two neurons (corresponding to temperature and conversion), the hidden layer containing five neurons, and the output layer containing one

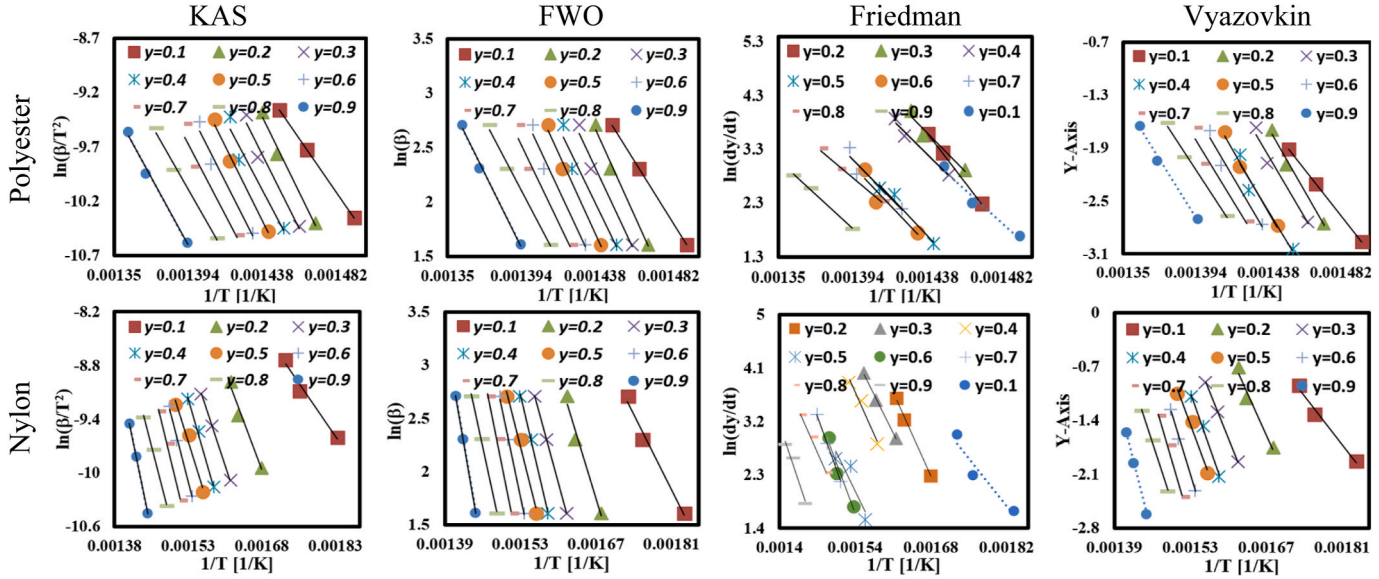

Figure (7). Linear and non-linear kinetic models fitting curves of plastic button catalytic pyrolysis.

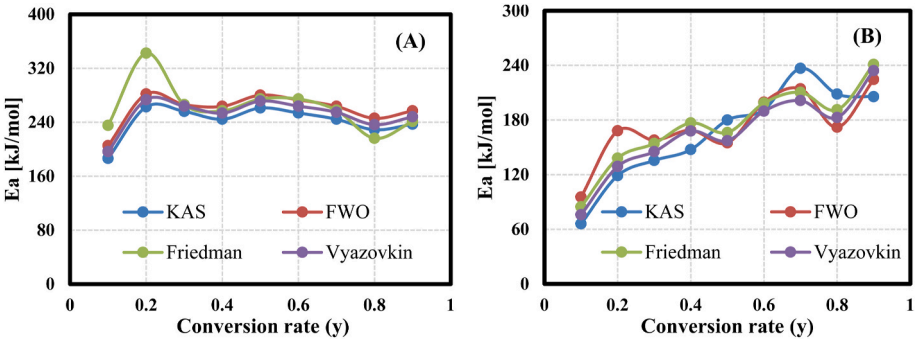

Figure (8). Ea distribution of A) polyester and B) nylon button samples.

Table (6)
Ea values of plastic button batches.

y	*KAS*		*FWO*		*Friedman*		*Vyazovkin*	
	Ea (KJ/mol)	R^2	*Ea* (KJ/mol)	R^2	*Ea* (KJ/mol)	R^2	*Ea* (KJ/mol)	R^2
Polyester buttons								
0.1	186.4	1.00	205.3	1.00	235.3	0.97	196.2	1.00
0.2	262.7	0.99	281.8	0.99	342.4	1.00	273.0	0.99
0.3	256.1	0.97	266.0	0.97	266.0	0.95	263.6	0.97
0.4	244.4	0.94	263.6	0.95	256.9	0.98	253.2	0.97
0.5	261.2	0.99	280.2	0.99	274.4	0.98	271.0	1.00
0.6	253.7	0.96	273.1	0.97	274.4	0.99	263.6	1.00
0.7	244.4	0.94	263.6	0.94	257.7	0.99	254.4	0.97
0.8	228.9	0.99	245.8	0.99	216.2	0.99	236.1	0.97
0.9	236.9	0.99	256.9	0.99	241.1	1.00	247.8	1.00
Avg.	241.6	0.98	259.6	0.98	262.7	0.98	251.0	0.98
Nylon buttons								
0.1	66.0	0.98	95.3	0.98	84.6	1.00	76.1	0.98
0.2	118.9	0.98	168.1	0.98	138.0	1.00	129.1	0.99
0.3	135.5	1.00	157.9	1.00	154.2	1.00	145.4	1.00
0.4	147.6	1.00	168.8	1.00	176.8	0.98	168.1	1.00
0.5	180.0	0.97	154.9	0.97	166.2	1.00	157.4	0.98
0.6	191.2	1.00	199.5	1.00	198.6	0.99	190.0	0.97
0.7	236.7	0.99	214.3	1.00	210.3	1.00	201.6	1.00
0.8	208.5	1.00	172.1	1.00	191.2	1.00	183.0	1.00
0.9	205.5	1.00	224.5	1.00	241.1	1.00	234.5	1.00
Avg.	165.6	0.99	172.8	0.99	173.4	1.00	165.0	0.99

neuron (representing the predicted activation energy or pyrolysis rate). This configuration was chosen after testing several layer arrangements and was found to provide the best generalization ability, as demonstrated by the excellent performance metrics in the attached results: R ≥ 0.99999 across training, validation, and test datasets, and very low MSE values (0.0038071 and 0.035867) as shown in Figure (9). Based on the optimized ANN algorithms, TGA curves were forecasted at a rate of 25 °C/min and subsequently compared to the experimental TGA results (Figure (10)). The results showed a good match within the permissible limits. These results demonstrate that artificial neural networks can act as an advanced model to predict catalytic thermochemical degradation of plastic buttons with high accuracy.

Finally, it would be useful to separate char against ZSM-5 zeolite catalyst and analyse the composition of char and its yield. However, this cannot be done using TGA (as an analytical reactor) due to the use of a very small amount of feedstock of buttons (less than 10 mg as mentioned in section 2.2). Since the residual mass was estimated at 20 wt%, this means that 1–2 mg remained, which is difficult to collect and separate, and not even sufficient for analysis using X-ray diffraction or scanning electron microscopy. Therefore, it is highly recommended for future work to conduct the catalytic pyrolysis experiments again using a small reactor that allows to get more residue in the end which helps to separate the char against the catalyst and distinguish both and calculate the yield as well.

4. Conclusions

In this examination, the catalytic thermochemical behavior of polyester and nylon button products was studied using TGA, while the vapors released from their decomposition were checked applying TG coupled with FTIR and GC/MS system. The detailed kinetic and thermogravimetric analysis of both samples were simulated through different traditional models along ANN as a modern machine learning tool. TGA measurements showed that both samples were almost completely decomposed up to 460 °C (polyester) and 490 °C (nylon) and carbonyl groups C=O and aliphatic hydrocarbons were the prevailing

Table (8)
Thermodynamic parameters of polyester button and nylon buttons.

Sample	Nylon (20 min/°C)			Polyester (10 min/°C)		
Parameter	ΔS (J/mol K)	ΔH (J/mol K)	ΔG (J/mol K)	ΔS (J/mol K)	ΔH (J/mol K)	ΔG (J/mol K)
KAS	−1335	−3451	577423	−1583	−3451	577423
FWO	−1433	−3444	620061	−1699	−3444	620061
FM	−1400	−3443	605595	−1660	−3443	605595

Table (7)
Ea of plastic button samples after several iterations.

y	Polyester				Nylon			
	First Iteration	second Iteration	third iteration	fourth iteration	First Iteration	second Iteration	third iteration	fourth iteration
0.1	196.5	196.8	196.5	196.5	76.1	76.1	76.1	76.1
0.2	273.3	273.4	273.4	273.4	129.2	129.1	129.1	129.1
0.3	264.5	264.6	263.9	263.9	145.5	145.4	145.4	145.4
0.4	254.9	349.6	253.6	253.6	168.1	168.1	168.1	168.1
0.5	271.4	271.4	271.4	271.4	157.3	157.4	157.4	157.4
0.6	264.3	264.3	263.9	263.9	190.0	190.0	190.0	190.0
0.7	255.2	254.7	254.7	254.7	201.5	201.6	201.6	201.6
0.8	236.9	236.9	236.4	236.4	174.8	182.8	183.0	183.0
0.9	248.1	241.4	248.1	248.1	234.4	234.5	234.5	234.5
Average	251.7	261.5	251.3	251.3	164.1	165.0	165.0	165.0

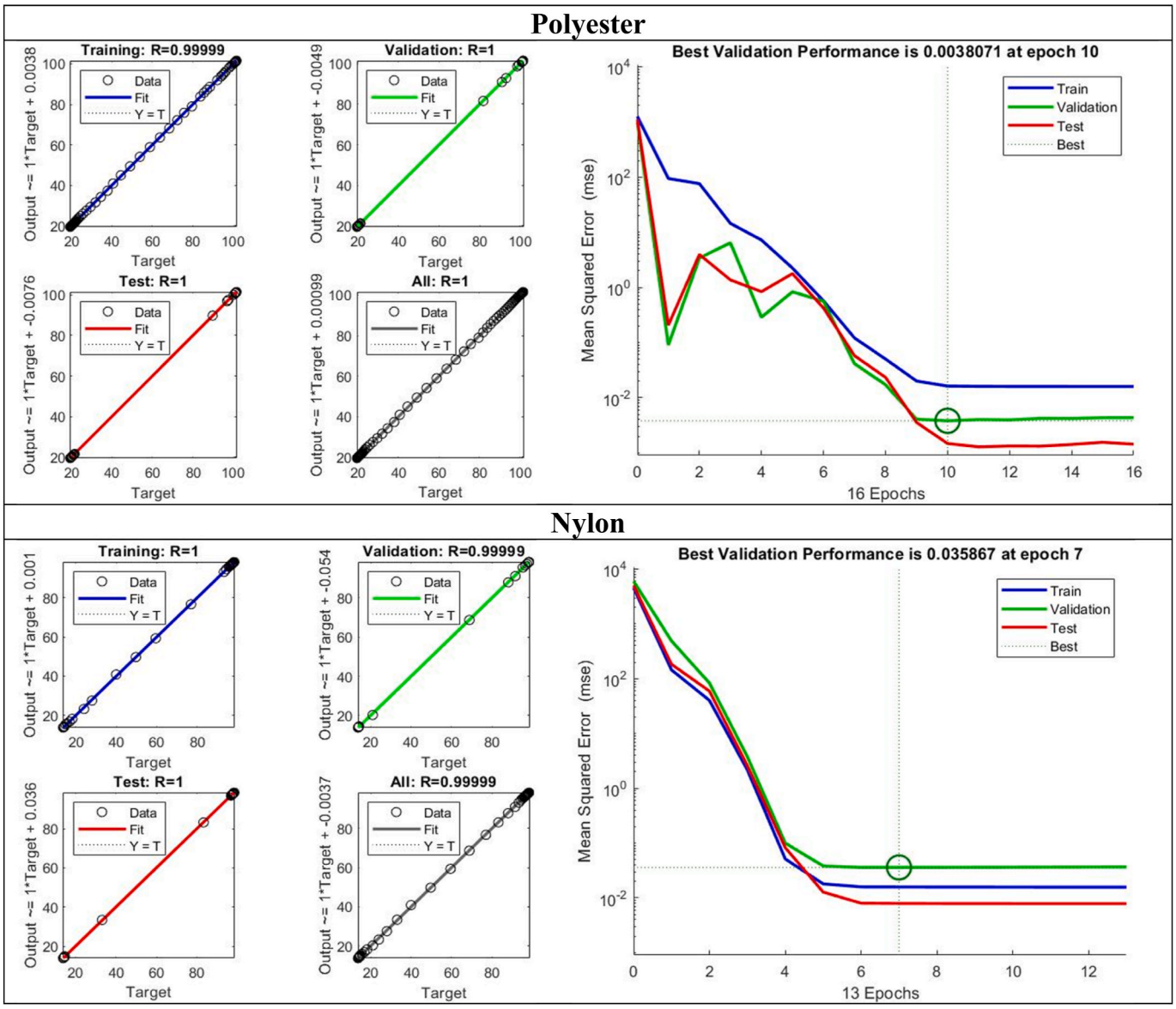

Figure (9). The ANN predicted charts of polyester and nylon button samples.

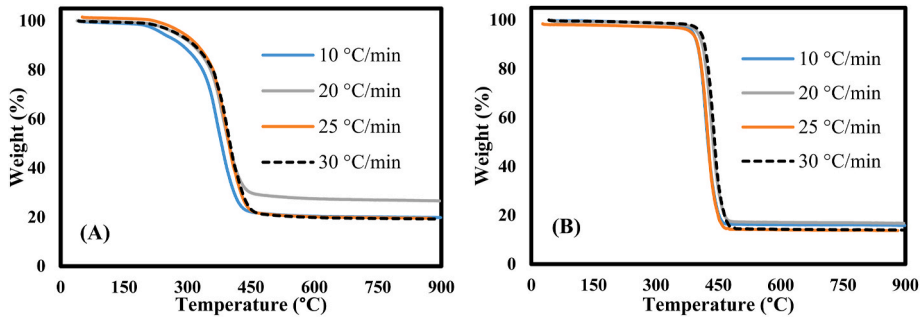

Figure (10). The measured TGA and ANN-forecasted data A) polyester and B) nylon button batches.

FTIR bands in the emitted catalytic vapors. The GC/MS observation process demonstrate that the main toxic compound of polyester (styrene) was eliminated and cleaved into its original chemicals like 1,2 Benzenedicarboxylic acid, Benzene, 1,1'-(1,3- propanediyl)bis-, etc. Similar in case of nylon, where its caprolactam has been decreased significantly (4.65 %) and cleaved into its original chemicals, in particular benzoic acid (up to 72.94 % at 20 min/°C). Finally, polyester buttons showed higher reaction complexity in terms of activation energy estimated at 241.6–262.7 kJ/mol versus 165.6–173.4 kJ/mol for nylon buttons. The proposed artificial neural network algorithm also successfully predicted the button samples decomposition characteristics for the training, validation and testing stages. Accordingly, the catalytic

thermochemical process is strongly advised to decompose buttons into their original chemical components used in their production.

CRediT authorship contribution statement

Samy Yousef: Writing – review & editing, Writing – original draft, Visualization, Validation, Supervision, Software, Resources, Project administration, Methodology, Investigation, Funding acquisition, Formal analysis, Data curation, Conceptualization. **Justas Eimontas:** Formal analysis, Data curation, Conceptualization, Resources. **Nerijus Striūgas:** Formal analysis, Data curation, Conceptualization, Resources. **Mohammed Ali Abdelnaby:** Software, Formal analysis, Data curation, Conceptualization.

Acknowledgment

This project has received funding from the Research Council of Lithuania (LMTLT), agreement No. S-MIP-23-118.

Data availability

The data that has been used is confidential.

References

[1] https://ec.europa.eu/commission/presscorner/detail/en/ip_23_3635.
[2] M. Solis, D. Tonini, C. Scheutz, L. Napolano, F. Biganzoli, D. Huygens, Contribution of waste management to a sustainable textile sector, Waste Manag. 189 (2024) 389–400, https://doi.org/10.1016/j.wasman.2024.08.037.
[3] B. Henry, K. Laitala, I.G. Klepp, Microfibres from apparel and home textiles: prospects for including microplastics in environmental sustainability assessment, Sci. Total Environ. 652 (2018) 483–494, https://doi.org/10.1016/j.scitotenv.2018.10.166.
[4] S.H. Akyildiz, H. Sezgin, B. Yalcin, I. Yalcin-Enis, Optimization of the textile wastewater pretreatment process in terms of organics removal and microplastic detection, J. Clean. Prod. 384 (2022) 135637, https://doi.org/10.1016/j.jclepro.2022.135637.
[5] S. Yousef, M. Tatariants, M. Tichonovas, L. Kliucininkas, S. Lukošiūtė, L. Yan, Sustainable green technology for recovery of cotton fibers and polyester from textile waste, J. Clean. Prod. 254 (2020) 120078, https://doi.org/10.1016/j.jclepro.2020.120078.
[6] R. Nayak, L. Jajpura, A. Khandual, Traditional Fibres for Fashion and Textiles: Associated Problems and Future Sustainable Fibres, Elsevier eBooks, 2023, pp. 3–25, https://doi.org/10.1016/b978-0-12-824052-6.00013-5.
[7] S. Yousef, M. Tatariants, M. Tichonovas, Z. Sarwar, I. Jonuškienė, L. Kliucininkas, A new strategy for using textile waste as a sustainable source of recovered cotton, Resour. Conserv. Recycl. 145 (2019) 359–369, https://doi.org/10.1016/j.resconrec.2019.02.031.
[8] K. Chatterjee, Y. Jhanji, T. Grover, N. Bansal, S. Bhattacharyya, Selecting Garment Accessories, Trims, and Closures, Elsevier eBooks, 2015, pp. 129–184, https://doi.org/10.1016/b978-1-78242-232-7.00006-0.
[9] S. Chand, S. Chand, B. Raula, Textile and apparel industries waste and its sustainable management approaches, J. Mater. Cycles Waste Manag. 25 (6) (2023) 3132–3143, https://doi.org/10.1007/s10163-023-01761-1.
[10] Iliana Papamichael, Irene Voukkali, Florentios Economou, Pantelitsa Loizia, Giorgos Demetriou, Mark Esposito, Vincenzo Naddeo, Marco Ciro Liscio, Paolo Sospiro, Antonis A. Zorpas, Mobilisation of textile waste to recover high added value products and energy for the transition to circular economy, Environ. Res. (2024), https://doi.org/10.1016/j.envres.2023.117716.
[11] Xinxin Huang, Yuhan Tan, Jiwei Huang, Guangzhou Zhu, Rong Yin, Xiaoming Tao, Xiao Tian, Industrialization of open- and closed-loop waste textile recycling towards sustainability: a review, J. Clean. Prod. (2024), https://doi.org/10.1016/j.jclepro.2024.140676.
[12] https://www.europarl.europa.eu/news/en/press-room/20240212IPR17625/textiles-and-food-waste-reduction-new-eu-rules-to-support-circular-economy.
[13] https://www.recycling-magazine.com/2023/07/07/trimclean-removes-trims-from-waste-textiles/.
[14] European Environment Agency. (2024), Overview of the capture rates for textiles and shoes per country, Retrieved from, https://www.eea.europa.eu/data-and-maps/figures/overview-of-the-capture-rates, 2020.
[15] Adewale S. Bello, Mohammad A. Al-Ghouti, Mohammed H. Abu-Dieyeh, Sustainable and long-term management of municipal solid waste: a review, Bioresour. Technol. Rep. (2022), https://doi.org/10.1016/j.biteb.2022.101067.
[16] X. Zhuang, N. Zhu, F. Li, H. Lin, C. Liang, Z. Dang, Y. Zou, Hydrogen-rich syngas production from waste textile gasification coupling with catalytic reforming under steam atmosphere, Processes 12 (9) (2024) 1790, https://doi.org/10.3390/pr12091790.
[17] L. Arjona, I.B. Gómez, Á.M. Salas, R.R. Solís, A.P. Muñoz, M.Á. Martín-Lara, G. Blázquez, M. Calero, Pyrolysis of textile waste: a SUSTAINABLE APPROACH TO WASTE MANAGEMENT AND RESOURCE RECOVERY, J. Environ. Chem. Eng. (2024) 114730, https://doi.org/10.1016/j.jece.2024.114730.
[18] P. Athanasopoulos, A. Zabaniotou, Post-consumer textile thermochemical recycling to fuels and biocarbon: a critical review, Sci. Total Environ. (2022), https://doi.org/10.1016/j.scitotenv.2022.155387.
[19] S. Yousef, J. Eimontas, N. Striūgas, M. Tatariants, M.A. Abdelnaby, S. Tuckute, L. Kliucininkas, A sustainable bioenergy conversion strategy for textile waste with self-catalysts using mini-pyrolysis plant, Energy Convers. Manag. 196 (2019) 688–704, https://doi.org/10.1016/j.enconman.2019.06.050.
[20] S. Yousef, M. Tatariants, M. Tichonovas, Z. Sarwar, I. Jonuškienė, L. Kliucininkas, A new strategy for using textile waste as a sustainable source of recovered cotton, Resour. Conserv. Recycl. 145 (2019) 359–369, https://doi.org/10.1016/j.resconrec.2019.02.031.
[21] M. Solis, D. Huygens, D. Tonini, T.F. Astrup, Management of textile waste in Europe: an environmental and a socio-economic assessment of current and future scenarios, Resour. Conserv. Recycl. 207 (2024) 107693, https://doi.org/10.1016/j.resconrec.2024.107693.
[22] S. Capuzzi, G. Timelli, Preparation and melting of scrap in aluminum recycling: a review, Metals 8 (4) (2018) 249, https://doi.org/10.3390/met8040249.
[23] X. Zhao, H. Ye, F. Chen, G. Wang, Bamboo as a substitute for plastic: research on the application performance and influencing mechanism of bamboo buttons, J. Clean. Prod. 446 (2024) 141297, https://doi.org/10.1016/j.jclepro.2024.141297.
[24] S. Yousef, J. Eimontas, N. Striūgas, M. Praspaliauskas, M.A. Abdelnaby, Pyrolysis behavior of non-textile components (buttons) and their kinetic analysis using artificial neural network, J. Anal. Appl. Pyrolysis (2024) 106880, https://doi.org/10.1016/j.jaap.2024.106880.
[25] A. Minor, R. Goldhahn, L. Rihko-Struckmann, K. Sundmacher, Chemical recycling processes of nylon 6 to caprolactam: review and techno-economic assessment, Chem. Eng. J. 474 (2023) 145333, https://doi.org/10.1016/j.cej.2023.145333.
[26] G. Scélo, V. Constantinescu, I. Csiki, D. Zaridze, N. Szeszenia-Dabrowska, P. Rudnai, J. Lissowska, E. Fabiánová, A. Cassidy, A. Slamova, L. Foretova, V. Janout, J. Fevotte, T. Fletcher, A.'. Mannetje, P. Brennan, P. Boffetta, Occupational exposure to vinyl chloride, acrylonitrile and styrene and lung cancer risk (Europe), Cancer Causes Control 15 (5) (2004) 445–452, https://doi.org/10.1023/b:caco.0000036444.11655.be.
[27] W. Yang, S. Jung, J. Lee, S.W. Lee, Y.T. Kim, E.E. Kwon, Selective recovery of caprolactam from the thermo-catalytic conversion of textile waste over γ-Al2O3 supported metal catalysts, Environ. Pollut. 329 (2023) 121684, https://doi.org/10.1016/j.envpol.2023.121684.
[28] J. Eimontas, S. Yousef, N. Striūgas, M.A. Abdelnaby, Catalytic pyrolysis kinetic behaviour and TG-FTIR-GC–MS analysis of waste fishing nets over ZSM-5 zeolite catalyst for caprolactam recovery, Renew. Energy 179 (2021) 1385–1403, https://doi.org/10.1016/j.renene.2021.07.143.
[29] S. Yousef, J. Eimontas, N. Striūgas, M.A. Abdelnaby, Synthesis of value-added aromatic chemicals from catalytic pyrolysis of waste wind turbine blades and their kinetic analysis using artificial neural network, J. Anal. Appl. Pyrolysis 177 (2023) 106330, https://doi.org/10.1016/j.jaap.2023.106330.
[30] J. Eimontas, N. Striūgas, M.A. Abdelnaby, Synthesis of benzoic acid from catalytic co-pyrolysis of waste wind turbine blades and biomass and their kinetic analysis, J. Anal. Appl. Pyrolysis 182 (2024) 106684, https://doi.org/10.1016/j.jaap.2024.106684.
[31] https://www.acsmaterial.com/zsm-5-catalyst.html.
[32] N. Striūgas, J. Eimontas, M.A. Abdelnaby, Co-pyrolysis of waste wind turbine blades and biomass and their kinetic analysis using artificial neural network, J. Anal. Appl. Pyrolysis 179 (2024) 106495, https://doi.org/10.1016/j.jaap.2024.106495.
[33] S. Yousef, J. Eimontas, K. Meile, N. Striūgas, M.A. Abdelnaby, Co-pyrolysis of Baltic wheat straw and low-density polyethylene bags and its kinetic and thermodynamic behaviour, Ind. Crop. Prod. 218 (2024) 118970, https://doi.org/10.1016/j.indcrop.2024.118970.
[34] M. Praspaliauskas, J. Eimontas, N. Striūgas, M.A. Abdelnaby, Pyrolysis kinetic behaviour, TG-FTIR, and GC/MS analysis of cigarette butts and their components, Biomass Convers. Bioref. 14 (5) (2022) 6903–6923, https://doi.org/10.1007/s13399-022-02698-5.
[35] J. Eimontas, N. Striūgas, M.A. Abdelnaby, S. Yousef, Catalytic pyrolysis kinetic behavior and TG-FTIR-GC–MS analysis of metallized food packaging plastics with different concentrations of ZSM-5 zeolite catalyst, Polymers 13 (5) (2021) 702, https://doi.org/10.3390/polym13050702.
[36] A. Mohamed, J. Eimontas, N. Striūgas, M.A. Abdelnaby, Pyrolysis kinetic behavior and TG-FTIR-GC–MS analysis of end-life ultrafiltration polymer nanocomposite membranes, Chem. Eng. J. 428 (2021) 131181, https://doi.org/10.1016/j.cej.2021.131181.
[37] S.P. Subadra, J. Eimontas, N. Striūgas, M.A. Abdelnaby, Thermal degradation and pyrolysis kinetic behaviour of glass fibre-reinforced thermoplastic resin by TG-FTIR, Py-GC/MS, linear and nonlinear isoconversional models, J. Mater. Res. Technol. 15 (2021) 5360–5374, https://doi.org/10.1016/j.jmrt.2021.11.011.
[38] S. Yousef, J. Eimontas, N. Striūgas, M.A. Abdelnaby, Pyrolysis and gasification kinetic behavior of mango seed shells using TG-FTIR-GC–MS system under N_2 and CO_2 atmospheres, Renew. Energy 173 (2021) 733–749, https://doi.org/10.1016/j.renene.2021.04.034.
[39] J. Eimontas, N. Striūgas, M.A. Abdelnaby, Pyrolysis kinetic behaviour and TG-FTIR-GC–MS analysis of Coronavirus face masks, J. Anal. Appl. Pyrolysis 156 (2021) 105118, https://doi.org/10.1016/j.jaap.2021.105118.

[40] S. Yousef, J. Eimontas, N. Striūgas, M.A. Abdelnaby, Influence of carbon black filler on pyrolysis kinetic behaviour and TG-FTIR-GC–MS analysis of glass fibre reinforced polymer composites, Energy 233 (2021) 121167, https://doi.org/10.1016/j.energy.2021.121167.
[41] K. Zakarauskas, J. Eimontas, N. Striūgas, M. Praspaliauskas, M.A. Abdelnaby, Pyrolysis kinetic behavior and TG-FTIR-GC–MS analysis of metallised food packaging plastics, Fuel 282 (2020) 118737, https://doi.org/10.1016/j.fuel.2020.118737.
[42] A. Mohamed, J. Eimontas, N. Striūgas, M.A. Abdelnaby, Pyrolysis behaviour of ultrafiltration polymer composite membranes (PSF/PET): kinetic, thermodynamic, prediction modelling using artificial neural network and volatile product analysis, Fuel 369 (2024) 131779, https://doi.org/10.1016/j.fuel.2024.131779.
[43] B. Gajera, U. Tyagi, A.K. Sarma, M.K. Jha, Pyrolysis of cattle manure: kinetics and thermodynamic analysis using TGA and artificial neural network, Biomass Convers. Bioref. 14 (19) (2023) 23605–23621, https://doi.org/10.1007/s13399-023-04476-3.
[44] A.M. Pannase, R.K. Singh, B. Ruj, P. Gupta, Decomposition of polyamide via slow pyrolysis: effect of heating rate and operating temperature on product yield and composition, J. Anal. Appl. Pyrolysis 151 (2020) 104886, https://doi.org/10.1016/j.jaap.2020.104886.
[45] S. Yousef, J. Eimontas, N. Striūgas, A. Mohamed, M.A. Abdelnaby, Pyrolysis kinetic behavior and thermodynamic analysis of PET nonwoven fabric, Materials 16 (18) (2023) 6079, https://doi.org/10.3390/ma16186079.
[46] Arantxa M. Gonzalez-Aguilar, Vicente Pérez-García, José M. Riesco-Ávila, A thermo-catalytic pyrolysis of polystyrene waste review: a systematic, statistical, and bibliometric approach, Polymers 15 (6) (2023) 1582, https://doi.org/10.3390/polym15061582.
[47] https://chemcess.com/industrial-production-of-%CE%B5-caprolactam/.
[48] J. Hong, X. Xu, Environmental impact assessment of caprolactam production – a case study in China, J. Clean. Prod. 27 (2012) 103–108, https://doi.org/10.1016/j.jclepro.2011.12.037.
[49] https://www.chemicalbook.com/Article/Application-and-Pharmacology-of-Benzoic-acid.htm.
[50] Homogeneous Catalysts. Activity—Stability—Deactivation. By PietW.N.M. vanLeeuwen and JohnC. Chadwick, Angew. Chem., Int. Ed. 51 (7) (2012) 1518. https://doi.org/10.1002/anie.201108293.
[51] K. Zakarauskas, J. Eimontas, N. Striūgas, Microcrystalline paraffin wax, biogas, carbon particles and aluminum recovery from metallised food packaging plastics using pyrolysis, mechanical and chemical treatments, J. Clean. Prod. 290 (2021) 125878, https://doi.org/10.1016/j.jclepro.2021.125878.
[52] N. Striūgas, J. Eimontas, M.A. Abdelnaby, Modeling of metalized food packaging plastics pyrolysis kinetics using an independent parallel reactions kinetic model, Polymers 12 (8) (2020) 1763, https://doi.org/10.3390/polym12081763.
[53] S. Yousef, J. Eimontas, N. Striūgas, M.A. Abdelnaby, Recovery of styrene from waste wind turbine blades (fiberglass/polyester resin composites) using pyrolysis treatment and its kinetic behavior, J. Therm. Anal. Calorim. 149 (2) (2023) 521–538, https://doi.org/10.1007/s10973-023-12714-z.
[54] H. Ryou, S.W. Kim, J. Byun, J. Han, J. Lee, Energy-efficient eco-friendly marine waste treatment: recovery of caprolactam from fishing net waste using seashell-derived catalyst, Energy 312 (2024) 133574, https://doi.org/10.1016/j.energy.2024.133574.
[55] S. Czernik, C.C. Elam, R.J. Evans, R.R. Meglen, L. Moens, K. Tatsumoto, Catalytic pyrolysis of nylon-6 to recover caprolactam, J. Anal. Appl. Pyrolysis 46 (1) (1998) 51–64, https://doi.org/10.1016/s0165-2370(98)00068-0.
[56] F. Yi, D. Xu, Z. Tao, C. Hu, Y. Bai, G. Zhao, H. Chen, J. Cao, Y. Yang, Correlation of Brønsted acid sites and Al distribution in ZSM-5 zeolites and their effects on butenes conversion, Fuel 320 (2022) 123729, https://doi.org/10.1016/j.fuel.2022.123729.
[57] H. Paysepar, K.T.V. Rao, Z. Yuan, H. Shui, C. Xu, Improving activity of ZSM-5 zeolite catalyst for the production of monomeric aromatics/phenolics from hydrolysis lignin via catalytic fast pyrolysis, Applied Catalysis a General 563 (2018) 154–162, https://doi.org/10.1016/j.apcata.2018.07.003.
[58] J. Wu, S. Wang, H. Li, Y. Zhang, R. Shi, Y. Zhao, The synergistic effect of acidic properties and channel systems of zeolites on the synthesis of polyoxymethylene dimethyl ethers from dimethoxymethane and trioxymethylene, Nanomaterials 9 (9) (2019) 1192, https://doi.org/10.3390/nano9091192.
[59] A.M. Gonzalez-Aguilar, V.P. Cabrera-Madera, J.R. Vera-Rozo, J.M. Riesco-Ávila, Effects of heating rate and temperature on the thermal pyrolysis of expanded polystyrene Post-Industrial waste, Polymers 14 (22) (2022) 4957, https://doi.org/10.3390/polym14224957.
[60] J.M. Riesco-Avila, J.R. Vera-Rozo, D.A. Rodríguez-Valderrama, D.M. Pardo-Cely, B. Ramón-Valencia, Effects of heating rate and temperature on the yield of thermal pyrolysis of a random waste plastic mixture, Sustainability 14 (15) (2022) 9026, https://doi.org/10.3390/su14159026.
[61] M. Safdari, E. Amini, D.R. Weise, T.H. Fletcher, Heating rate and temperature effects on pyrolysis products from live wildland fuels, Fuel 242 (2019) 295–304, https://doi.org/10.1016/j.fuel.2019.01.040.
[62] B. Zhao, D. O'Connor, J. Zhang, T. Peng, Z. Shen, D.C. Tsang, D. Hou, Effect of pyrolysis temperature, heating rate, and residence time on rapeseed stem derived biochar, J. Clean. Prod. 174 (2017) 977–987, https://doi.org/10.1016/j.jclepro.2017.11.013.
[63] S. Yousef, J. Eimontas, K. Zakarauskas, N. Striūgas, I. Pitak, Catalytic reforming of tar for enhancing hydrogen production from gasification of hazardous medical waste, Energy 313 (2024) 134184, https://doi.org/10.1016/j.energy.2024.134184.
[64] M.M. Harussani, S.M. Sapuan, Umer Rashid, A. Khalina, R.A. Ilyas, Pyrolysis of polypropylene plastic waste into carbonaceous char: priority of plastic waste management amidst COVID-19 pandemic, Sci. Total Environ. (2022), https://doi.org/10.1016/j.scitotenv.2021.149911.
[65] S. Yousef, J. Eimontas, N. Striūgas, A. Mohamed, M.A. Abdelnaby, Morphology, compositions, thermal behavior and kinetics of pyrolysis of lint-microfibers generated from clothes dryer, J. Anal. Appl. Pyrolysis 155 (2021) 105037, https://doi.org/10.1016/j.jaap.2021.105037.
[66] A.C.M. Loy, S. Yusup, B.S. How, C.L. Yiin, B.L.F. Chin, M. Muhammad, Y.L. Gwee, Uncertainty estimation approach in catalytic fast pyrolysis of rice husk: thermal degradation, kinetic and thermodynamic parameters study, Bioresour. Technol. 294 (2019) 122089, https://doi.org/10.1016/j.biortech.2019.122089.
[67] I. Kiminaitė, J. Eimontas, N. Striūgas, M.A. Abdelnaby, Catalytic pyrolysis kinetic behaviour of glass fibre-reinforced epoxy resin composites over ZSM-5 zeolite catalyst, Fuel 315 (2022) 123235, https://doi.org/10.1016/j.fuel.2022.123235.
[68] Z. Zhang, Y. Li, L. Luo, D. Yellezuome, M.M. Rahman, J. Zou, H. Hu, J. Cai, Insight into kinetic and thermodynamic analysis methods for lignocellulosic biomass pyrolysis, Renew. Energy 202 (2022) 154–171, https://doi.org/10.1016/j.renene.2022.11.072.